GABA release selectively regulates synapse development at distinct inputs on direction-selective retinal ganglion cells

Adam Bleckert[a,1], Chi Zhang[a,1], Maxwell H. Turner[b], David Koren[c], David M. Berson[d], Silvia J. H. Park[e], Jonathan B. Demb[e,f], Fred Rieke[b,g], Wei Wei[c,2], and Rachel O. Wong[a,2]

[a]Department of Biological Structure, University of Washington, Seattle, WA 98195; [b]Department of Physiology and Biophysics, University of Washington, Seattle, WA 98195; [c]Department of Neurobiology, University of Chicago, Chicago, IL 60637; [d]Department of Neuroscience, Brown University, Providence, RI 02912; [e]Department of Ophthalmology and Visual Science, Yale University, New Haven, CT 06511; [f]Department of Cellular and Molecular Physiology, Yale University, New Haven, CT 06511; and [g]Howard Hughes Medical Institute, University of Washington, Seattle, WA 98195

Edited by Joshua R. Sanes, Harvard University, Cambridge, MA, and approved November 2, 2018 (received for review February 27, 2018)

Synaptic inhibition controls a neuron's output via functionally distinct inputs at two subcellular compartments, the cell body and the dendrites. It is unclear whether the assembly of these distinct inhibitory inputs can be regulated independently by neurotransmission. In the mammalian retina, γ-aminobutyric acid (GABA) release from starburst amacrine cells (SACs) onto the dendrites of on–off direction-selective ganglion cells (ooDSGCs) is essential for directionally selective responses. We found that ooDSGCs also receive GABAergic input on their somata from other amacrine cells (ACs), including ACs containing the vasoactive intestinal peptide (VIP). When net GABAergic transmission is reduced, somatic, but not dendritic, $GABA_A$ receptor clusters on the ooDSGC increased in number and size. Correlative fluorescence imaging and serial electron microscopy revealed that these enlarged somatic receptor clusters are localized to synapses. By contrast, selectively blocking vesicular GABA release from either SACs or VIP ACs did not alter dendritic or somatic receptor distributions on the ooDSGCs, showing that neither SAC nor VIP AC GABA release alone is required for the development of inhibitory synapses in ooDSGCs. Furthermore, a reduction in net GABAergic transmission, but not a selective reduction from SACs, increased excitatory drive onto ooDSGCs. This increased excitation may drive a homeostatic increase in ooDSGC somatic $GABA_A$ receptors. Differential regulation of $GABA_A$ receptors on the ooDSGC's soma and dendrites could facilitate homeostatic control of the ooDSGC's output while enabling the assembly of the GABAergic connectivity underlying direction selectivity to be indifferent to altered transmission.

activity-dependent synapse development | GABA receptors | retinal development | amacrine cells

In addition to its central role in mature circuits, neurotransmission plays critical roles in shaping neuronal connectivity patterns during development. Excitatory neurotransmission has a well-established role in regulating multiple aspects of circuit development (1, 2), and classic inhibitory neurotransmitters, such as GABA, likely play important roles as well (3). Inhibitory neurotransmission does not appear to be essential for the initial clustering of inhibitory receptors but instead can influence the correct targeting and organization of receptors and scaffolding proteins at inhibitory synaptic sites (4–10). Moreover, presynaptic specializations including axonal bouton number and size are also susceptible to the blockade of GABAergic transmission (11). However, a comprehensive understanding of the role of GABA-mediated transmission in circuit development is still lacking because perturbing GABAergic transmission can have disparate effects on inhibitory synapse development across different circuits. For instance, early visual deprivation has opposite effects on the amplitude of the inhibitory synaptic inputs that fast-spiking and regular-spiking inhibitory interneurons provide to layer 4 cortical pyramidal cells (12). Moreover, suppressing GABAergic transmission from cortical basket cells using genetic knockout of either GABA-synthesizing enzymes (GAD67 or GAD65) or the vesicular inhibitory amino acid transporter (VIAAT) (13, 14) stabilizes some basket cell synapses while facilitating the elimination of others (15). GABAergic synapses at different cell compartments or bearing different receptor subunit compositions also appear differentially sensitive to the loss of GABAergic transmission during development (10, 16, 17).

What factors underlie the apparently distinctive actions of inhibitory neurotransmission on the development and maturation of inhibitory synapses? The complexity of neuronal circuits often makes it difficult to tease apart these factors because most individual postsynaptic cells receive converging input from multiple types of inhibitory interneurons at synapses with different compositions of receptor types or targeted to different subcellular locations. Here, we focused on a well-studied and relatively compact microcircuit of the mouse retina for motion processing (18–20) to determine whether distinct sets of feedforward GABAergic synapses on the same postsynaptic neuron are

Significance

Output characteristics of a neuron are shaped by synaptic inhibition onto its soma and dendrites. These subcellular compartments of direction-selective retinal ganglion cells (DSGCs) receive input from different types of inhibitory neurons, and only dendritic inhibition generates the DSGC's direction selectivity. Perturbing γ-aminobutyric acid (GABA) release either at all or at selected GABAergic inputs uncovered differential roles for GABAergic transmission on synaptic development at the DSGC's soma and dendrites. Although dendritic $GABA_A$ receptor clustering is largely invariant to transmission loss, somatic receptor clusters can increase in number and size. These findings advance our understanding of the roles of activity-dependent and -independent mechanisms in the development of inhibitory inputs that play separate roles in controlling the output of an individual neuron.

Author contributions: A.B., C.Z., M.H.T., D.K., D.M.B., S.J.H.P., J.B.D., F.R., W.W., and R.O.W. designed research; A.B., C.Z., M.H.T., D.K., D.M.B., S.J.H.P., J.B.D., F.R., W.W., and R.O.W. performed research; A.B., C.Z., M.H.T., D.K., D.M.B., S.J.H.P., J.B.D., F.R., W.W., and R.O.W. contributed new reagents/analytic tools; A.B., C.Z., M.H.T., D.M.B., F.R., W.W., and R.O.W. analyzed data; and A.B., C.Z., M.H.T., D.M.B., S.J.H.P., J.B.D., F.R., W.W., and R.O.W. wrote the paper.

The authors declare no conflict of interest.

This article is a PNAS Direct Submission.

[1]A.B. and C.Z. contributed equally to this work.

[2]To whom correspondence may be addressed. Email: weiw@uchicago.edu or wongr2@u.washington.edu.

This article contains supporting information online at www.pnas.org/lookup/suppl/doi:10.1073/pnas.1803490115/-/DCSupplemental.

Published online December 3, 2018.

regulated together or separately during development. Although the presynaptic inhibitory neurons are distinct, their contacts are made at postsynaptic sites with $GABA_A$ receptors ($GABA_A$Rs) comprising the same α and γ subunits, thus removing diverse receptor subtypes as a factor. Genetic tools also allow us to manipulate distinct inhibitory synapses selectively in this retinal microcircuit.

The direction-selective ganglion cell (DSGC) responds most robustly to movement along a preferred direction and is least responsive to movement in the opposite (or null) direction (21). This response feature is shaped by inhibitory input onto the dendrites of the DSGC primarily from GABAergic starburst amacrine cells (SACs) (22). However, inhibitory currents that persist upon specific deletion of VIAAT expression in SACs suggest that other GABAergic amacrine cells (ACs) contact the on–off DSGC (ooDSGC) (23). We identified GABAergic innervation from other AC types, including vasoactive intestinal peptide (VIP)-expressing ACs, on ooDSGC somata. The somatic synapses on DSGCs express $GABA_A$Rs, which, like those on their dendrites, contain α2 subunits. We bred Cre-recombinase driver lines with floxed (fl) VIAAT mice (*Slc32a1*$^{fl/fl}$) (24) to perturb either all GABAergic transmission onto the DSGC or only the inhibitory input from the SACs or VIP ACs. This approach enabled us to ascertain whether $GABA_A$Rs of the same type but at distinct cellular compartments or synapses of the postsynaptic cell are regulated similarly or independently by neurotransmission. Moreover, we were able to distinguish the role of GABA release in the development of inhibitory inputs that contribute in different ways toward defining the ooDSGC output.

Results

Transgenic Disruption of GABAergic Neurotransmission and Visualization of Retinal $GABA_A$Rs. To confine the loss of inhibitory neurotransmission to the retina, we generated a retina-specific knockout of VIAAT by breeding *Slc32a1*$^{fl/fl}$ mice with mice expressing Cre-recombinase under the control of the retina-specific promoter *αPax6-Cre-IRES-GFP* (25), henceforth referred to as "VIAAT^{KO}" mice. The unique pattern of Cre-recombinase expression in the retina results in a relatively greater loss of VIAAT, as assessed by VIAAT immunostaining, in nasal and temporal retina than in a dorsal-to-ventral strip of retina (Fig. 1 *A*–*C*). Note, however, that within a Cre-expressing region most, but not all, ACs express Cre-recombinase; thus VIAAT expression persists in some ACs (Fig. 1*B*). To compare $GABA_A$R distribution on ganglion cells (GCs) with normal inhibition and on GCs with perturbed inhibition, we imaged and analyzed GCs in either the central control (Cre^-) regions of VIAAT^{KO} retina or Cre^- littermate control (VIAAT$^+$) retinas versus GCs located within the nasal and temporal (Cre^+) regions of VIAAT^{KO} retinas.

To visualize GABAergic postsynaptic sites, we crossed the VIAAT^{KO} mice with *Thy1-YFPγ2* mice in which the γ2 subunit of $GABA_A$Rs is tagged with YFP (26). The γ2 subunit is necessary for synaptic localization of $GABA_A$Rs (27). GABAergic synapses

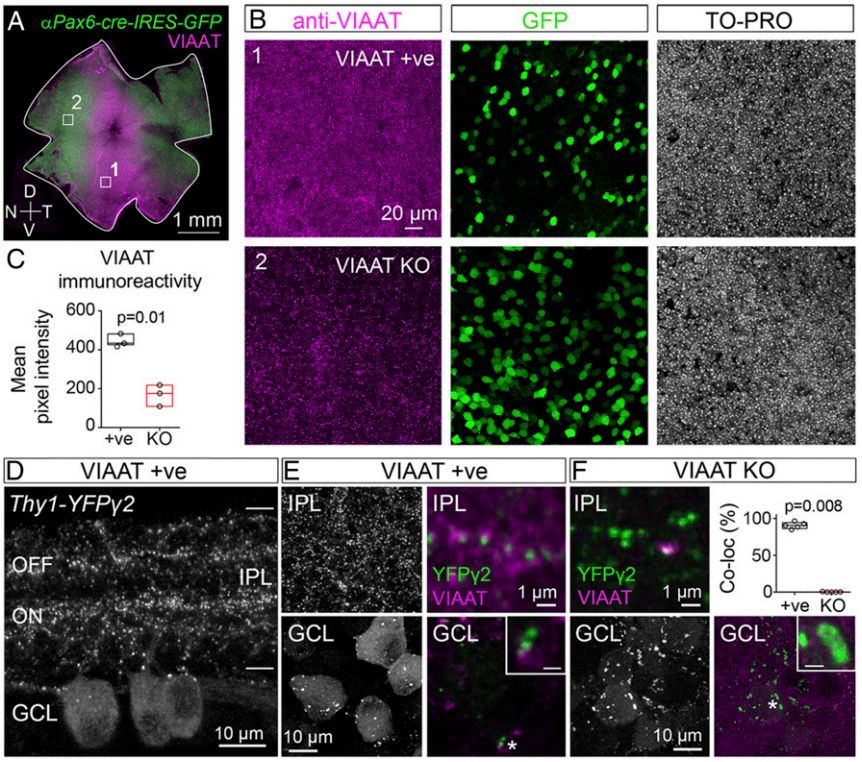

Fig. 1. *YFPγ2* expression at GABAergic synapses in control and VIAAT^{KO} retinas. (*A*) VIAAT expression is highly reduced in the nasal and temporal regions of the VIAAT^{KO} retina, where a greater proportion of ACs express *αPax6-Cre-IRES-GFP*. Box 1 is a region with high VIAAT expression (control region); box 2 is a region with low VIAAT expression (KO region). D, dorsal; N, nasal; T, temporal; V, ventral. (*B*) VIAAT expression in the IPL (*Left*), in Cre-expressing ACs labeled by GFP in the INL (*Center*), and in INL cell nuclei stained by TO-PRO (Thermo-Fisher) (*Right*) within the regions outlined by Box 1 (control) and Box 2 (KO) in *A*. (*C*) Mean pixel intensity of VIAAT immunoreactivity in control (+ve) and KO regions of the same retinas (paired *t* test; $n = 3$ retinas). (*D*) Vertical section through a *Thy1-YFPγ2* retina showing the distribution of GABARs fused to YFP (YFPγ2) in the IPL and GCL. Two bands of YFPγ2 puncta at the stratification levels of the ON and OFF SAC processes were evident. Faint YFP fluorescence in cell bodies represents the intracellular pools of the tagged receptors. (*E*) In VIAAT$^+$ retina, YFPγ2 puncta in the IPL (*Upper Row*) and on the soma of retinal ganglion cells (*Lower Row*) are apposed to VIAAT$^+$ puncta. (*Inset*) A magnified view of the contact indicated by the asterisk. (*F*, *Upper Left*) In VIAAT^{KO} retina, some VIAAT$^+$ processes persist but were rarely juxtaposed to YFPγ2 puncta. (*Upper Right*) The colocalization plot shows somatic YFPγ2 puncta in the GCL (*Bottom Row*) are rarely apposed to VIAAT$^+$ profiles compared with VIAAT$^+$ control regions ($n = 5$ regions from each of two retinas). (*Inset*) A magnified view of a somatic receptor cluster marked by the asterisk in the *Bottom Right* image.

on ~50% of GCs were visualized in these transgenic mice, and dense expression was observed particularly within an ON and an OFF plexus in the inner plexiform layer (IPL) corresponding to the stratification of the ON and OFF cholinergic SAC processes (Fig. 1 *D* and *E*, IPL) (26). Somata in the ganglion cell layer (GCL) were also decorated with YFPγ2 puncta (Fig. 1*E*, GCL). Immunostaining for VIAAT confirmed that YFPγ2 puncta in both the IPL and the GCL are normally apposed to $VIAAT^{+}$ presynaptic puncta (Fig. 1*E*). In $VIAAT^{KO}$ mice, some VIAAT-labeled terminals were apposed to YFPγ2 puncta throughout the IPL (Fig. 1*F*, IPL), but none was apposed to YFPγ2 puncta on the somata (Fig. 1*F*). This suggests that in these knockout retinas GABA release onto GC dendrites is reduced but not completely abolished, whereas release onto the soma is severely diminished (Fig. 1 *E* and *F*).

Effects on $GABA_A$γ2 Receptors on ooDSGCs in the $VIAAT^{KO}$ Vary Across Cell Compartments. Some, but not all, GC somata have larger YFPγ2 clusters in the $VIAAT^{KO}$ (Fig. 1*F*, GCL and *SI Appendix*, Fig. S1). Enlarged clusters were not apparent at postnatal day (P) 11 but became prominent by P21. Because not all GC somata within a field of view have abnormally large YFPγ2 puncta, we assessed which type or types of GCs in the $VIAAT^{KO}$ were affected. To label the GCs, we biolistically transfected retinas from control *Thy1-YFPγ2* animals and *Thy1-YFPγ2*/$VIAAT^{KO}$ mice with CMV-tdTomato. GC types were identified based on their dendritic morphology and stratification patterns within the IPL (20). Ten of ten cells with dendritic morphology characteristic of ooDSGCs (19, 28) demonstrated large receptor clusters on their cell bodies (Fig. 2 *A*–*D*), whereas wide-field ON-α GCs within the same region appeared unaffected (*SI Appendix*, Fig. S1*C*).

We next determined whether the dendritic arbors of ooDSGCs were perturbed in the $VIAAT^{KO}$. We found that ooDSGCs maintained bistratified dendritic arbors ramifying in both ON and OFF plexuses, and neither the total dendritic length nor the total number of dendritic segments changed as a result of reduced inhibition (Fig. 2*E*). The branching patterns of ooDSGCs, determined by Sholl analysis (29), were also similar to those in wild-type mice (Fig. 2*E*). Thus, overall, dendritic development of ooDSGCs was not affected in the $VIAAT^{KO}$, in contrast to turtle GCs, whose dendritic development was affected when GABAergic transmission was blocked pharmacologically (30). We next compared the distribution of YFPγ2 puncta on the dendrites and somata of the ooDSGC in $VIAAT^{KO}$ and control retinas. We skeletonized the tdTomato cell fill and mapped the somatic and dendritic postsynaptic sites labeled by YFPγ2 expression (*SI Appendix*). We found that the median number of YFPγ2 puncta on ooDSGC somata almost doubled and the median volume of the inhibitory somatic contacts almost tripled in the $VIAAT^{KO}$ retinas (Fig. 2*F*), resulting from a skew in the distribution toward larger-volume YFPγ2 clusters (Fig. 2*F*). In contrast, the median linear density of YFPγ2 puncta on the ooDSGC dendrites showed a modest decrease in the $VIAAT^{KO}$, with no change to the volume of dendritic YFPγ2 clusters (Fig. 2*G*). Thus, diminishing GABA release resulted in differential effects on γ2-containing $GABA_A$Rs on the soma and dendrites of the ooDSGCs.

Enlarged Somatic YFPγ2 Puncta Colocalize with Other Inhibitory Postsynaptic Proteins. The prominent clusters on ooDSGC somata could represent aggregates of nonsynaptic receptors (9, 31). We thus determined whether somatic YFPγ2 puncta in $VIAAT^{+}$ retina colocalize with gephyrin, a postsynaptic scaffolding protein found at GABAergic and glycinergic synapses in the retina (32). Indeed, somatic YFPγ2 puncta normally colocalized with gephyrin (*SI Appendix*, Fig. S2). Likewise, the enlarged somatic YFPγ2 puncta in the $VIAAT^{KO}$ also colocalized with gephyrin. Furthermore, in both $VIAAT^{+}$ and $VIAAT^{KO}$ backgrounds, somatic YFPγ2 overlapped with the α2 subunit of the $GABA_A$R, which is known to be an essential component of inhibitory synaptic receptors on ooDSGCs (*SI Appendix*, Fig. S2) (33). In $VIAAT^{KO}$ mice without the Thy1-YFP*γ2* transgene, immunostaining for gephyrin or the $GABA_A$R α2 subunit also revealed enlarged somatic puncta (*SI Appendix*, Fig. S2), suggesting that these large YFPγ2 clusters were not explained by overexpression of YFPγ2. Collectively, these observations suggest that the abnormally large somatic YFPγ2 puncta in the $VIAAT^{KO}$ are likely to be at genuine postsynaptic sites. However, to confirm that this is so, we performed correlative light and serial electron microscopy to determine whether presynaptic structures are apposed to the somatic YFPγ2 puncta.

Presynaptic Terminals Are Apposed to YFPγ2 Puncta on ooDSGC Somata. Synaptic connectivity is most reliably defined at the ultrastructural level. To perform correlative fluorescence imaging of the somatic YFPγ2 clusters with serial block face scanning electron microscopy (SBFSEM), we used the near-infrared branding technique (26, 34) to make fiducial marks on the retina (35). After registration of the fluorescence image with the SEM micrographs (Fig. 3 *A* and *B*), we segmented and reconstructed the ooDSGCs (two $VIAAT^{+}$ and three $VIAAT^{KO}$ cells) and traced the processes that contacted the GC soma (Fig. 3 *B*–*D*). These processes terminated over YFPγ2 clusters (Fig. 3*B*), contained vesicles, and contacted the GC soma at sites with postsynaptic densities (see examples in Fig. 3*E*). Presynaptic terminals apposed to the three largest YFPγ2 puncta (Fig. 3 *C* and *D*, white arrowheads) fasciculated with the primary dendrite before forming a terminal varicosity opposite an enlarged somatic YFPγ2 punctum (Fig. 3 *C* and *D*, black arrowheads). The remaining connections associated with the smaller YFPγ2 puncta did not contact the ooDSGC's primary dendrites but directly contacted the soma. Somatic AC contacts were also present on ooDSGCs in control retina, suggesting that they were not formed ectopically when GABA release was diminished (*SI Appendix*, Fig. S3).

Because the type or types of ACs contacting ooDSGC somata are unknown, we reconstructed the ACs that synapsed onto the ooDSGCs (n = 4 cells), using a second SBFSEM dataset (36). We found that ooDSGCs are contacted by at least two types of ACs, one with morphology resembling bistratified VIP-expressing ACs (37–39) and the other with morphology resembling the type 52 AC of Helmstaedter et al. (40) (Fig. 3 *F*–*L* and *SI Appendix*, Fig. S4). Because not all the ACs contacting the ooDSGCs could be traced fully, there may be additional AC types that provide somatic input.

Disrupting SAC- or VIP AC-Mediated Inhibition Does Not Alter Somatic $GABA_A$R Clustering. We next sought to understand better the cellular basis for the differential effects of perturbed inhibitory transmission on $GABA_A$R clusters on the somata and on the dendrites of ooDSGCs. We first selectively removed dendritic inhibition from SACs that provide the major inhibitory drive to the ooDSGC (23). This was achieved by crossing *ChAT-ires-cre* mice with the *slc32a1*$^{fl/fl}$ mice to produce mice that we term "$VIAAT^{ChATsp\text{-}KO}$ mice." Immunostaining for VIAAT in $VIAAT^{ChATsp\text{-}KO}$ retinas confirmed a selective loss of VIAAT in the choline acetyltransferase (ChAT) bands in the IPL (*SI Appendix*, Fig. S6*A*). ooDSGCs were intracellularly dye-filled in the retinas of both wild-type and the $VIAAT^{ChATsp\text{-}KO}$ mice, and their $GABA_A$Rs were revealed by YFPγ2 expression or by immunostaining for the α2 subunit of the $GABA_A$R or for gephyrin. As in the $VIAAT^{KO}$, receptor clusters on the dendrites appeared qualitatively normal in size (Fig. 4*A*). The density of $GABA_A$R clusters on the dendrites was not significantly different from that of control retinas. Receptor and gephyrin clusters on the cell somata of the $VIAAT^{ChATsp\text{-}KO}$ mice were also unchanged (Fig. 4 *B* and *C*). Somatic YFPγ2 puncta on the

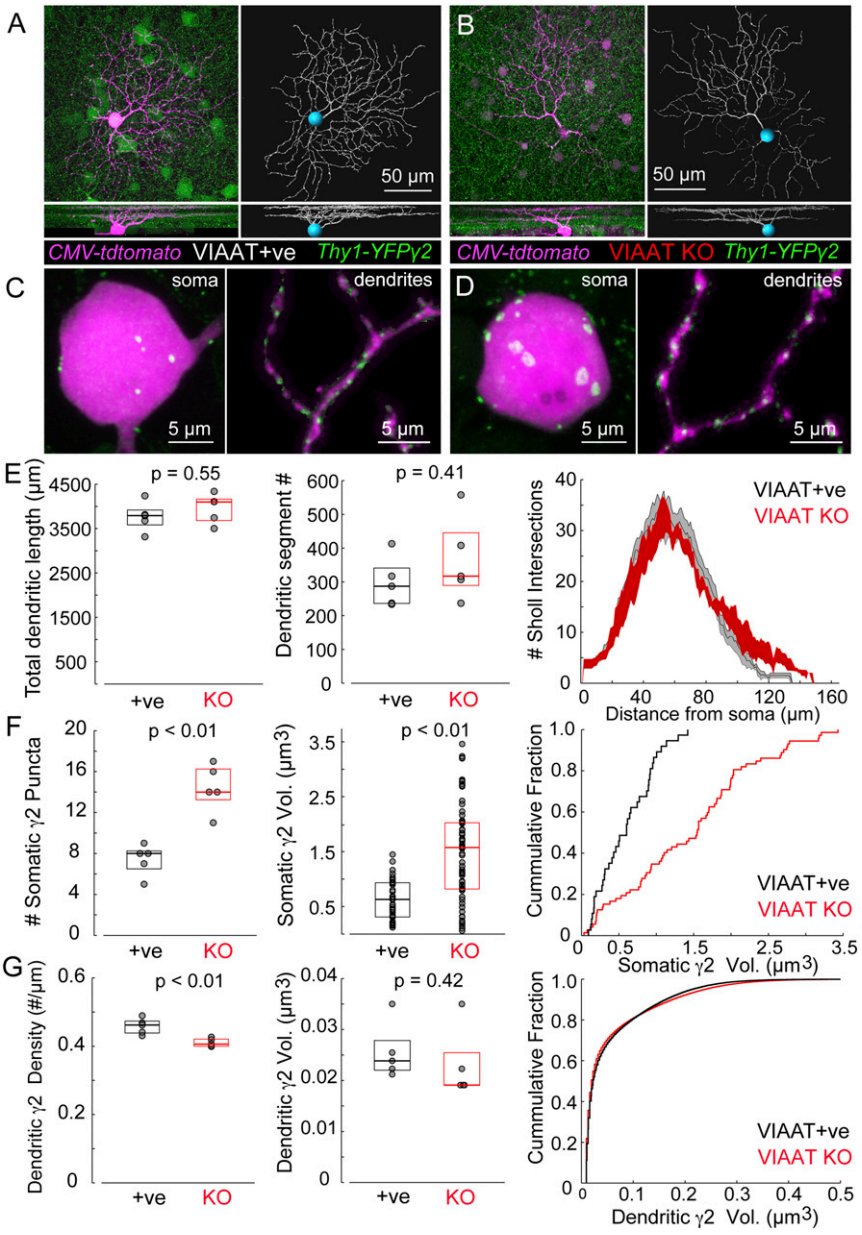

Fig. 2. Large YFPγ2 perisomatic puncta are found on bistratified direction-selective GCs. (*A–D*) Perisomatic but not dendritic YFPγ2 clusters were enlarged in the bistratified ooDSGCs following VIAAT knockout. (*A* and *B*, *Left*) Maximum intensity projections of the dendritic arbors of an ooDSGC biolistically transfected with *CMV-tdTomato* in *Thy1-YFPγ2* retina in control or in *VIAAT*^{KO} backgrounds. In *A*, the imaging area was reduced at the level of the cell body to reduce the time for image acquisition; both the dendrites and the soma were acquired at the same pixel resolution within a single image stack. In *B*, the *en face* view is a maximum intensity projection of the image planes encompassing the dendrites only; the sideview is a projection of the entire image stack. (*Right*) Skeletonized filaments of the dendritic arbors. Orthogonal rotations of the images are provided below. (*C* and *D*) Magnified views of YFPγ2 on ooDSGC somata and dendrites of cells in *A* and *B*, respectively. (*E*) Total dendritic length, total dendritic segment number, and number of Sholl branch intersections versus distance from the soma for ooDSGCs from control [VIAAT^{+} (+ve); $n = 5$ cells] and VIAAT^{KO} (KO; $n = 5$ cells) retinas. (*F*) Median number, median volume, and cumulative distribution of the perisomatic YFPγ2 puncta. Control (*Thy1-YFPγ2*) values in *E* and *F* are replotted from ref. 26. (*G*) Linear density, median volume, and cumulative distribution of YFPγ2 puncta on ooDSGC dendrites.

VIAAT$^{ChATsp\text{-}KO}$ mice ($n = 5$ cells) showed no significant differences from controls in mean count (Fig. 4*D*) or mean puncta size (Fig. 4*E*). Thus, loss of SAC inhibition on the ooDSGCs does not significantly perturb the dendritic or somatic $GABA_AR$ distributions on these GCs.

To gain a better understanding of how VIAAT removal changes excitatory and inhibitory inputs onto ooDSGCs, we measured light responses of ooDSGCs in VIAAT^{KO} and VIAAT$^{ChATsp\text{-}KO}$ retinas. The incomplete removal of VIAAT in VIAAT^{KO} retinas precludes a comparison of responses across the two lines; instead, we compared the responses of knockouts and controls within each line separately.

In the VIAAT^{KO}, we targeted ooDSGCs in the nasal–temporal regions of the retina where enlarged YFPγ2 puncta were visible and filled the cells with dye to confirm their identity after whole-cell recording. We compared the light responses of these cells with those of ooDSGCs from VIAAT^{+} retinal regions or from littermate control retinas. We found a significant reduction

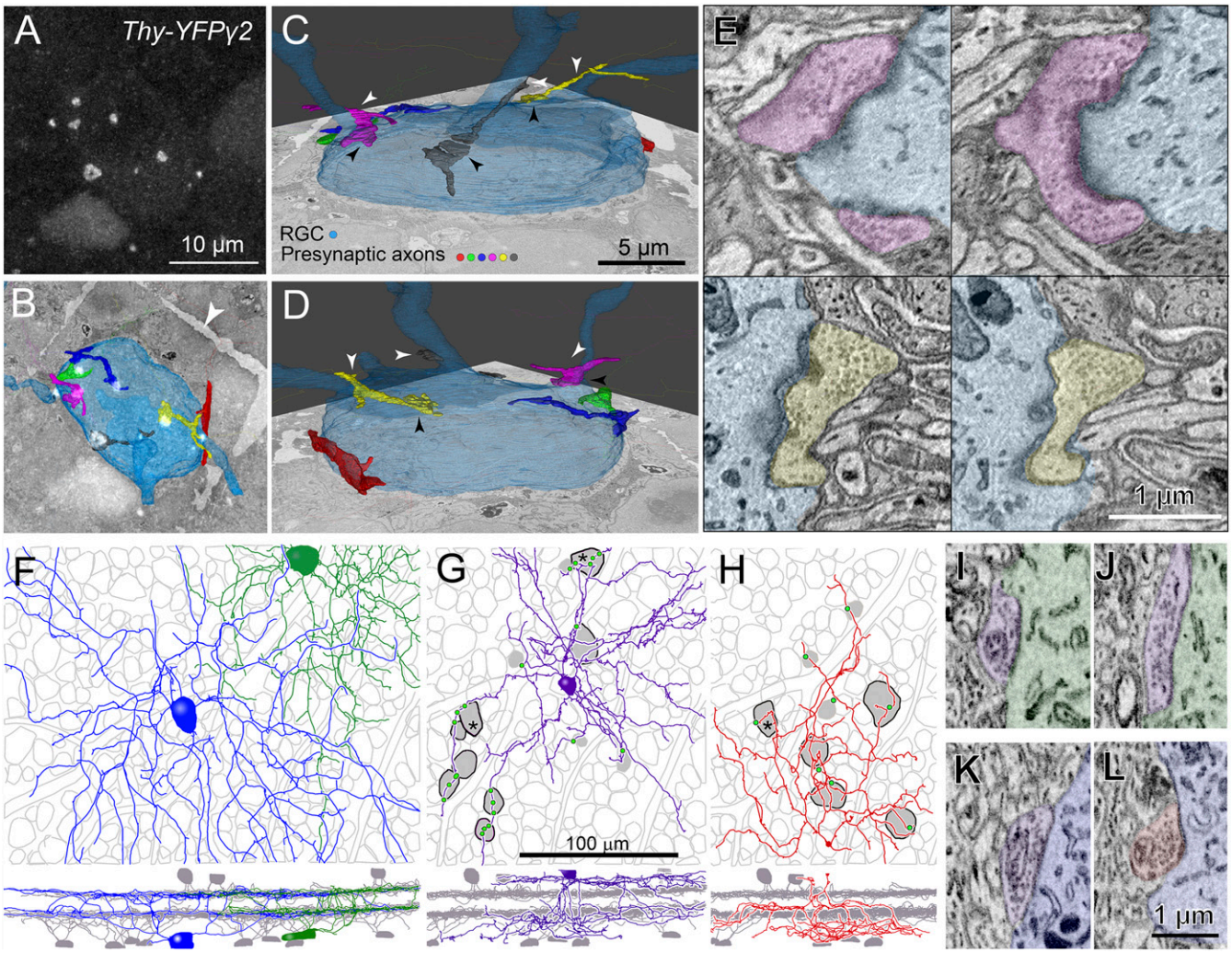

Fig. 3. Inhibitory synapses are present at enlarged perisomatic receptor clusters on ooDSGCs in VIAAT^{KO} retina. (*A*) YFPγ2 puncta onto an ooDSGC. (*B*) Overlay of YFPγ2 fluorescence from *A* and SBFSEM reconstruction of the ooDSGC soma identified by near-infrared burned fiducial marks (arrowhead). Axon terminals from ACs are colored separately. (*C* and *D*) Front (*C*) and rear (*D*) views of the reconstructed volume from *B* show three AC processes (burgundy, magenta, and yellow) that make initial contact and fasciculate with the primary dendritic arbors of the ooDSGC (white arrowheads) before terminating on the soma (black arrowheads). The other three presynaptic terminals (red, blue, and green) do not contact the ooDSGC's primary dendrites. (*E*) Consecutive sections showing two somatic contacts. (*F–L*) ACs making axosomatic contacts onto ooDSGCs in a larger SBFSEM volume. (*F–H*) Reconstructions of several synaptically connected neurons. (*F*) Two ooDSGCs. (*G*) A presumed bistratified VIP AC. (*H*) A type 52 AC. Each cell is shown *en face* (*Upper*) with somas and vessels of the ganglion cell layer (gray outlines) and in side view (*Lower*) along with gray cholinergic bands revealed by numerous reconstructed SACs. In *G* and *H*, axosomatic contacts from the ACs are marked by green dots. Somata receiving those contacts are shaded gray; a black outline indicates a GC; the others are ACs. Asterisks in *G* and *H* mark the two ooDSGCs in *F*. (*I–L*) Examples of axosomatic contacts. Profiles are tinted to match the color scheme in *F–H*. Contacts of the VIP AC onto both ooDSGCs are seen in *I–K*; the contact from the type 52 AC to one of the ooDSGCs appears in *L*. Reprinted by permission from ref. 36, Springer Nature: Nature, copyright (2016).

in inhibitory charge transfer for ooDSGCs in VIAAT^{KO} retinas. The recorded cells still possessed a direction-selective response (*SI Appendix*, Fig. S5), consistent with incomplete excision of VIAAT in the IPL leading to residual inhibitory input to ooDSGCs from the SACs. A previous study (23) showed that direction selectivity is severely reduced in ooDSGCs in VIAAT$^{ChATsp\text{-}KO}$ retinas, and paired SAC-ooDSGC recordings and responses to moving bars confirmed that inhibitory input from the SACs is indeed markedly diminished but not completely eliminated (*SI Appendix*, Fig. S6 *B* and *C*). Interestingly, excitatory charge transfer increased in the VIAAT^{KO} but not in VIAAT$^{ChATsp\text{-}KO}$ retinas (*SI Appendix*, Figs. S5*D* and S6*D*), likely because bipolar cell inputs were disinhibited upon the global disruption of GABA and glycine release from ACs other than the SACs.

Finally, we crossed *VIP-ires-cre* mice with *slc32a1$^{fl/fl}$* mice to remove VIAAT expression selectively from VIP ACs and asked if this would lead to an increase in size in their postsynaptic sites on the ooDSGC somata. VIP ACs were visualized by crossing in a Cre-dependent channel rhodopsin-2/EYFP reporter allele (Ai32 mice), which results in fluorescent labeling of the membrane (39). We performed gephyrin immunolabeling to visualize the $GABA_AR$s and CART immunolabeling to identify DSGCs. DSGCs and R-type GCs are labeled by anti-CART but are distinguished by their disparate soma size (41). VIAAT staining confirmed that the YFP-labeled VIP terminals did not contain VIAAT (*SI Appendix*, Fig. S7). There were no enlarged clusters opposite VIP YFP$^+$ terminals on CART-labeled somata (Fig. 4 *F* and *G*). Thus, perturbing inhibition from VIP ACs alone does

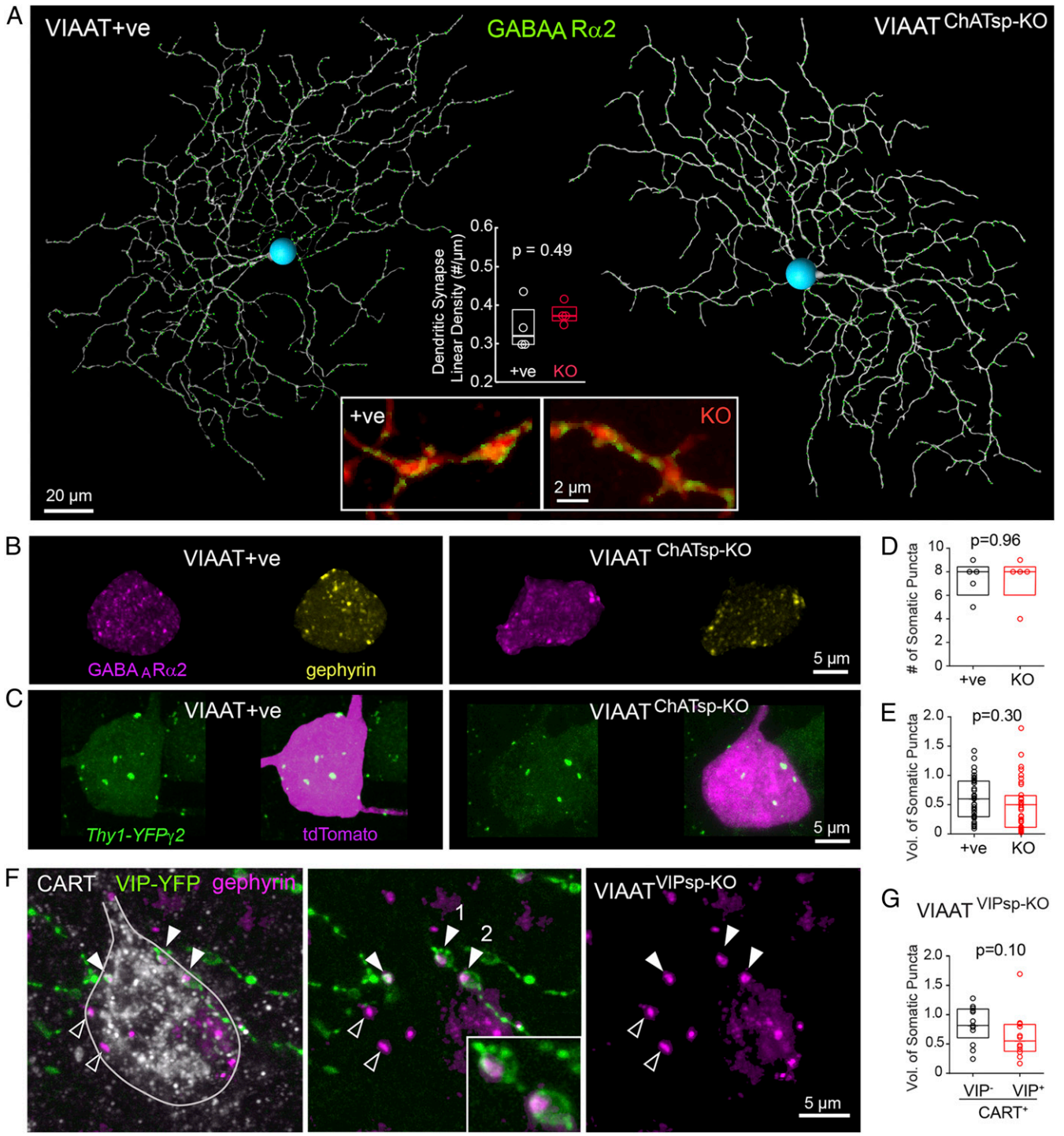

Fig. 4. Selective blockade of GABAergic transmission from SACs or VIP ACs does not perturb YFPγ2 puncta arrangements on ooDSGC soma and dendrites. (*A*) Distributions of YFPγ2 puncta (green dots) on skeletonized dendritic arbors of ooDSGCs in control (VIAAT^{+}) and SAC-specific VIAAT$^{ChATsp\text{-}KO}$. (*Insets*) Raw images of the dendrites labeled upon intracellular dye-filling with Lucifer yellow (red) and immunostaining for GABA$_A$Rα2 subunits. Dendritic GABA$_A$Rα2 puncta (synapse) density is provided in the plot ($n = 4$ cells each). (*B*) Examples of GABA$_A$Rα2 and gephyrin immunolabeling on the soma of an ooDSGC, identified after intracellular dye-filling in control (VIAAT^{+}, $n = 4$ cells) and KO ($n = 4$ cells) animals. (*C*) Examples of YFPγ2 clusters on the somata of ooDSGCs in control and VIAAT$^{ChATsp\text{-}KO}$ retinas. (*D* and *E*) Somatic YFPγ2 puncta density (*D*) and size (*E*) are not affected by selective knockout of VIAAT in SACs ($n = 5$ cells each). Control values in *D* and *E* are replotted from ref. 26. (*F*) A CART-labeled ooDSGC (outlined by the thin white line) in VIP VIAAT$^{VIPsp\text{-}KO}$ retina, showing somatic inhibitory synapses (labeled by gephyrin) that are apposed to VIP (filled arrowheads; labeled by cre-dependent YFP expression) and non-VIP (open arrowheads) terminals. (*Inset*) Magnified view of VIP boutons 1 and 2. (*G*) Volume of gephyrin^{+} puncta opposite YFP-expressing VIP AC boutons (VIP^{+}) versus puncta associated with other AC types (VIP^{-}) ($n = 5$ cells each).

not cause an enlargement of $GABA_AR$ clusters at synapses with DSGCs or across somatic synapses with other AC types.

Discussion

A Previously Unidentified Set of Inhibitory Synapses on ooDSGCs. The role of synaptic inhibition in the retina has best been defined for the circuitry that underlies direction selectivity. Direction selectivity in ooDSGCs arises from the asymmetric inhibition of SACs and the GC dendrites (22, 42–46). By expressing YFP-tagged γ2 subunits of the $GABA_AR$ in GCs and performing correlative fluorescence imaging and SBFSEM, we uncovered a set of GABAergic synapses on the somata of the ooDSGCs. We found that these GABAergic postsynaptic sites on ooDSGC somata contain gephyrin and the $GABA_AR$ α2 subunit. The α2 subunit is also the α subunit localized at SAC synapses on the dendrites of the ooDSGCs (33). Thus, ooDSGCs do not utilize different $GABA_AR$ subunit combinations to segregate and encode inputs from distinct types of presynaptic amacrine cells.

Previous electron microscopy reconstruction of cat β cells showed that inhibitory somatic contacts may originate from a single type of GABAergic AC (47). However, we show here that mouse ooDSGCs receive input onto their somata from two or more types of ACs, one of which resembles a bistratified VIP AC (37–39) and another that resembles the type 52 AC (40). Previous electrophysiological recordings from ooDSGCs in the absence of SAC GABAergic drive revealed the presence of sustained weaker and non–direction-selective inhibitory currents (23); these currents may reflect somatic inhibition, a possibility that remains to be tested.

Disrupting GABA Release Produces Contrasting Alterations to Dendritic and Somatic GABAergic Synapses on ooDSGCs. Perturbing GABA release has been found previously to affect the development of GABAergic synapses on different compartments of the postsynaptic cell differently. For example, knocking out the α2 subunit of $GABA_ARs$ selectively disrupts GABAergic synapses onto the somata of hippocampal pyramidal neurons, whereas synapses onto the dendrites are unaffected (48). Similar knockout of specific subunits of $GABA_ARs$ (16, 49) can also result in disparate effects on synaptic connectivity onto Purkinje cell dendrites, somata, and axon initial segments. Likewise, $GABA_ARs$ with different subunit compositions on the axons and dendrites of bipolar cells in the $VIAAT^{KO}$ mouse retina demonstrate different sensitivities to the loss of GABAergic transmission in the during development (10). The differential dependence on GABA release may arise because GABA synapses at different cell compartments are often composed of different receptor subunits (50). However, in the present study, differences in the composition of $GABA_A$ subunit are unlikely to explain the differential changes in receptor clustering on the dendrites and somata of the ooDSGCs in the $VIAAT^{KO}$ because α2γ2-containing receptors and their scaffolding protein gephyrin are present in both cellular compartments.

A key result of our study is that the loss of inhibitory input selectively from SACs or across all sources of GABAergic input causes little change in $GABA_AR$ distributions on ooDSGC dendrites. Our observations support previous findings in which the development of direction selectivity is not impaired by in vivo pharmacological blockade of $GABA_ARs$ in the developing mouse retina (51, 52). The small reduction in dendritic GABAergic synapse density on the ooDSGCs in the $VIAAT^{KO}$ is consistent with the loss of GABAergic synapses observed in visual cortex following either GAD67 knockout (15, 53) or perturbed visual activity (54). Because we did not find a significant change in the density of $GABA_AR$ clusters when VIAAT was selectively knocked out in SACs, it may be that the slight decrease observed in the $VIAAT^{KO}$ is due to a reduction of non-SAC dendritic GABAergic synapses. In either case, our current findings support the view that GABA release from SACs is not critical for the formation of their synapses with ooDSGCs. Therefore, the development of SAC–ooDSGC inhibitory synapses, which are necessary for establishing the directional selectivity of ooDSGCs, are resilient to changes in GABAergic transmission.

Unlike the dendritic receptors, somatic $GABA_AR$ clusters increase in number and size in the $VIAAT^{KO}$ but are not affected upon selective loss of vesicular GABA release from either SACs contacting the dendrites or VIP ACs contacting the ooDSGC soma. We think that somal location per se is not a major factor, because not all GC types showed enlarged somatic $GABA_AR$ clusters in the $VIAAT^{KO}$. Instead, we favor the possibility that the increase in somatic $GABA_AR$ clustering in ooDSGCs is in response to an increase in net excitation to these GCs in the $VIAAT^{KO}$ but not in the $VIAAT^{ChATsp\text{-}KO}$ retina. However, we cannot rule out the possibility that the differential effects on receptor clustering are AC-type specific.

In the absence of GABA release from presynaptic terminals, prominent developmental alterations in somatic inhibitory synapses of ooDSGCs differ sharply from the robust development of SAC–ooDSGC dendritic synapses. We postulate that the activity-dependent development of somatic inhibition serves to stabilize the firing rates of ooDSGCs, while activity-independent development of dendritic inhibition preserves the anatomical substrate (SAC connectivity) of the feature selectivity of ooDSGCs. Together, these compartment-specific developmental mechanisms ensure the emergence of reliable and robust computation of the retinal direction-selective circuit, making it invulnerable to the variability of activity levels that ooDSGCs might receive during development. Functions of ooDSGC somatic inhibition, including potential gain control of the ooDSGC response, remain to be elucidated.

The pronounced increase in the number of somatic inhibitory synapses on ooDSGCs in the $VIAAT^{KO}$ resembles findings from visual cortex where conditional knockout of VIAAT in basket cells resulted in an increase in the connections these inhibitory interneurons make onto pyramidal cell somata (15). However, basket cell terminal boutons onto cortical pyramidal cell somata are smaller when basket cells lack VIAAT or the synthesizing enzymes for GABA (15, 53). It is posited that the decreased size and increased number of somatic contacts from basket cells result from the persistence of nascent immature synapses, which normally are eliminated during development. In contrast, changes in the size and density of somatic receptor clusters on the ooDSGCs do not appear to be a consequence of a failure to reduce inhibitory somatic synapses during development, because we did not observe an overabundance of somatic contacts onto ooDSGCs during development in control animals. This discrepancy in observations from the cortex and retina could be due in part to the different approaches used to manipulate GABAergic transmission (1). Moreover, in previous work, GABAergic transmission from an individual basket cell contacting the pyramidal neuron is disrupted, leaving input from neighboring basket cells intact (3), whereas in the $VIAAT^{KO}$ retina all AC contacts onto the ooDSGC soma lacked VIAAT. It may be that competition between the different inhibitory inputs causes a reduction in the synapse size of interneurons with perturbed transmission, but when all inputs are affected the sizes of the receptor clusters increase to compensate homeostatically for the overall loss in inhibition and for the increased excitation.

Further investigation is needed to understand the role of activity in regulating the development and maturation of inhibitory circuits and why the development of some, but not all, GABAergic synapses depends on GABA release. Together with past studies, however, our current findings support the emerging view that activity-dependent mechanisms, which shape the development and maturation of inhibitory synapses, are complex and can operate independently at the level of individual input types or may be

engaged as part of a homeostatic attempt at a specific cell compartment to prevent runaway excitation of the postsynaptic cell.

Materials and Methods

All procedures were conducted with approval of the Institutional Animal Care and Use Committees at the University of Washington, the University of Chicago, and Yale University. Transgenic mouse line information is provided in *SI Appendix*.

Immunohistochemistry and Cell Labeling. Retinas were fixed in 4% paraformaldehyde for immunohistochemistry or after biolistic transfection with CMV-tdTomato. Primary antibodies used include anti-VIAAT, gephyrin, GAD67, $GABA_AR$ α2, ChAT, and CART. Drd4-GFP^+ ooDSGCs were targeted (45) and filled with Lucifer yellow CH (Thermo Fisher Scientific) and Alexa-Fluor 488 (Thermo Fisher Scientific). For further details, see *SI Appendix*.

Fluorescence Image Acquisition and Analysis. Confocal image stacks were analyzed using Fiji (NIH), Imaris (Bitplane), and MATLAB (MathWorks). See *SI Appendix* for details of image acquisition and analysis.

Correlative Fluorescence and Electron Microscopy. Correlative fluorescence and electron microscopy were performed as described previously (26). See *SI Appendix* for details.

Statistical Analysis. All data are shown as median box plots with edges demarcating the 25th and 75th percentiles, unless otherwise stated. A two-sided Wilcoxon rank sum test was used for the analysis.

ACKNOWLEDGMENTS. We thank Ed Parker for electron microscopy assistance. This work was funded by NIH Grants EY10699 (to R.O.W.), EY024016 (to W.W.), EY01730 (Vision Core, M. Neitz, Principal Investigator), EY014454 (to J.B.D.), EY026878 (Vision Core, M. Crair, Principal Investigator), NIH EY12793 (to D.M.B.), EY011850 (to F.R.), F31-EY026288 (to M.H.T.), and F30EY025958 (to D.K.) and by the Howard Hughes Medical Institute (F.R.).

1. Bleckert A, Wong RO (2011) Identifying roles for neurotransmission in circuit assembly: Insights gained from multiple model systems and experimental approaches. *Bioessays* 33:61–72.
2. Hong YK, Chen C (2011) Wiring and rewiring of the retinogeniculate synapse. *Curr Opin Neurobiol* 21:228–237.
3. Huang ZJ (2009) Activity-dependent development of inhibitory synapses and innervation pattern: Role of GABA signalling and beyond. *J Physiol* 587:1881–1888.
4. Brünig I, Suter A, Knuesel I, Lüscher B, Fritschy JM (2002) GABAergic terminals are required for postsynaptic clustering of dystrophin but not of GABA(A) receptors and gephyrin. *J Neurosci* 22:4805–4813.
5. Schweizer C, et al. (2003) The gamma 2 subunit of GABA(A) receptors is required for maintenance of receptors at mature synapses. *Mol Cell Neurosci* 24:442–450.
6. Lévi S, Logan SM, Tovar KR, Craig AM (2004) Gephyrin is critical for glycine receptor clustering but not for the formation of functional GABAergic synapses in hippocampal neurons. *J Neurosci* 24:207–217.
7. Christie SB, Li RW, Miralles CP, Yang B, De Blas AL (2006) Clustered and non-clustered GABAA receptors in cultured hippocampal neurons. *Mol Cell Neurosci* 31:1–14.
8. Patrizi A, et al. (2008) Synapse formation and clustering of neuroligin-2 in the absence of GABAA receptors. *Proc Natl Acad Sci USA* 105:13151–13156.
9. Poulopoulos A, et al. (2009) Neuroligin 2 drives postsynaptic assembly at perisomatic inhibitory synapses through gephyrin and collybistin. *Neuron* 63:628–642.
10. Hoon M, et al. (2015) Neurotransmission plays contrasting roles in the maturation of inhibitory synapses on axons and dendrites of retinal bipolar cells. *Proc Natl Acad Sci USA* 112:12840–12845.
11. Fu Y, Wu X, Lu J, Huang ZJ (2012) Presynaptic GABA(B) receptor regulates activity-dependent maturation and patterning of inhibitory synapses through dynamic allocation of synaptic vesicles. *Front Cell Neurosci* 6:57.
12. Maffei A, Nelson SB, Turrigiano GG (2004) Selective reconfiguration of layer 4 visual cortical circuitry by visual deprivation. *Nat Neurosci* 7:1353–1359.
13. McIntire SL, Reimer RJ, Schuske K, Edwards RH, Jorgensen EM (1997) Identification and characterization of the vesicular GABA transporter. *Nature* 389:870–876.
14. Chaudhry FA, et al. (1998) The vesicular GABA transporter, VGAT, localizes to synaptic vesicles in sets of glycinergic as well as GABAergic neurons. *J Neurosci* 18:9733–9750.
15. Wu X, et al. (2012) GABA signaling promotes synapse elimination and axon pruning in developing cortical inhibitory interneurons. *J Neurosci* 32:331–343.
16. Frola E, et al. (2013) Synaptic competition sculpts the development of GABAergic axodendritic but not perisomatic synapses. *PLoS One* 8:e56311.
17. Schubert T, Hoon M, Euler T, Lukasiewicz PD, Wong RO (2013) Developmental regulation and activity-dependent maintenance of GABAergic presynaptic inhibition onto rod bipolar cell axonal terminals. *Neuron* 78:124–137.
18. Weng S, Sun W, He S (2005) Identification of ON-OFF direction-selective ganglion cells in the mouse retina. *J Physiol* 562:915–923.
19. Wei W, Feller MB (2011) Organization and development of direction-selective circuits in the retina. *Trends Neurosci* 34:638–645.
20. Sanes JR, Masland RH (2015) The types of retinal ganglion cells: Current status and implications for neuronal classification. *Annu Rev Neurosci* 38:221–246.
21. Barlow HB, Levick WR (1965) The mechanism of directionally selective units in rabbit's retina. *J Physiol* 178:477–504.
22. Vaney DI, Sivyer B, Taylor WR (2012) Direction selectivity in the retina: Symmetry and asymmetry in structure and function. *Nat Rev Neurosci* 13:194–208.
23. Pei Z, et al. (2015) Conditional knock-out of vesicular GABA transporter gene from starburst amacrine cells reveals the contributions of multiple synaptic mechanisms underlying direction selectivity in the retina. *J Neurosci* 35:13219–13232.
24. Tong Q, Ye CP, Jones JE, Elmquist JK, Lowell BB (2008) Synaptic release of GABA by AgRP neurons is required for normal regulation of energy balance. *Nat Neurosci* 11:998–1000.
25. Marquardt T, et al. (2001) Pax6 is required for the multipotent state of retinal progenitor cells. *Cell* 105:43–55.
26. Bleckert A, et al. (2013) Spatial relationships between GABAergic and glutamatergic synapses on the dendrites of distinct types of mouse retinal ganglion cells across development. *PLoS One* 8:e69612.
27. Essrich C, Lorez M, Benson JA, Fritschy JM, Lüscher B (1998) Postsynaptic clustering of major GABAA receptor subtypes requires the gamma 2 subunit and gephyrin. *Nat Neurosci* 1:563–571.
28. Triplett JW, et al. (2014) Dendritic and axonal targeting patterns of a genetically-specified class of retinal ganglion cells that participate in image-forming circuits. *Neural Dev* 9:2.
29. Sholl DA (1953) Dendritic organization in the neurons of the visual and motor cortices of the cat. *J Anat* 87:387–406.
30. Chabrol FP, Eglen SJ, Sernagor E (2012) GABAergic control of retinal ganglion cell dendritic development. *Neuroscience* 227:30–43.
31. Saiepour L, et al. (2010) Complex role of collybistin and gephyrin in GABAA receptor clustering. *J Biol Chem* 285:29623–29631.
32. Sassoè-Pognetto M, Wässle H (1997) Synaptogenesis in the rat retina: Subcellular localization of glycine receptors, GABA(A) receptors, and the anchoring protein gephyrin. *J Comp Neurol* 381:158–174.
33. Auferkorte ON, et al. (2012) GABA(A) receptors containing the α2 subunit are critical for direction-selective inhibition in the retina. *PLoS One* 7:e35109.
34. Bishop D, Nikic I, Kerschensteiner M, Misgeld T (2014) The use of a laser for correlating light and electron microscopic images in thick tissue specimens. *Methods Cell Biol* 124:323–337.
35. Denk W, Horstmann H (2004) Serial block-face scanning electron microscopy to reconstruct three-dimensional tissue nanostructure. *PLoS Biol* 2:e329.
36. Ding H, Smith RG, Poleg-Polsky A, Diamond JS, Briggman KL (2016) Species-specific wiring for direction selectivity in the mammalian retina. *Nature* 535:105–110.
37. Pérez de Sevilla Müller L, et al. (May 4, 2017) Multiple cell types form the VIP amacrine cell population. *J Comp Neurol*, 10.1002/cne.24234.
38. Zhu Y, Xu J, Hauswirth WW, DeVries SH (2014) Genetically targeted binary labeling of retinal neurons. *J Neurosci* 34:7845–7861.
39. Park SJ, et al. (2015) Function and circuitry of VIP+ interneurons in the mouse retina. *J Neurosci* 35:10685–10700.
40. Helmstaedter M, et al. (2013) Connectomic reconstruction of the inner plexiform layer in the mouse retina. *Nature* 500:168–174.
41. Sabbah S, Berg D, Papendorp C, Briggman KL, Berson DM (2017) A Cre mouse line for probing irradiance- and direction-encoding retinal networks. *eNeuro* 4:ENEURO.0065-17.2017.
42. Briggman KL, Helmstaedter M, Denk W (2011) Wiring specificity in the direction-selectivity circuit of the retina. *Nature* 471:183–188.
43. Fried SI, Münch TA, Werblin FS (2002) Mechanisms and circuitry underlying directional selectivity in the retina. *Nature* 420:411–414.
44. Vlasits AL, et al. (2016) A role for synaptic input distribution in a dendritic computation of motion direction in the retina. *Neuron* 89:1317–1330.
45. Wei W, Elstrott J, Feller MB (2010) Two-photon targeted recording of GFP-expressing neurons for light responses and live-cell imaging in the mouse retina. *Nat Protoc* 5:1347–1352.
46. Yonehara K, et al. (2011) Spatially asymmetric reorganization of inhibition establishes a motion-sensitive circuit. *Nature* 469:407–410.
47. Kolb H, Nelson R (1993) OFF-alpha and OFF-beta ganglion cells in cat retina: II. Neural circuitry as revealed by electron microscopy of HRP stains. *J Comp Neurol* 329:85–110.
48. Panzanelli P, et al. (2011) Distinct mechanisms regulate GABAA receptor and gephyrin clustering at perisomatic and axo-axonic synapses on CA1 pyramidal cells. *J Physiol* 589:4959–4980.
49. Fritschy JM, Panzanelli P, Kralic JE, Vogt KE, Sassoè-Pognetto M (2006) Differential dependence of axo-dendritic and axo-somatic GABAergic synapses on GABAA receptors containing the alpha1 subunit in Purkinje cells. *J Neurosci* 26:3245–3255.
50. Kasugai Y, et al. (2010) Quantitative localisation of synaptic and extrasynaptic GABAA receptor subunits on hippocampal pyramidal cells by freeze-fracture replica immunolabelling. *Eur J Neurosci* 32:1868–1888.
51. Wei W, Hamby AM, Zhou K, Feller MB (2011) Development of asymmetric inhibition underlying direction selectivity in the retina. *Nature* 469:402–406.
52. Sun L, Han X, He S (2011) Direction-selective circuitry in rat retina develops independently of GABAergic, cholinergic and action potential activity. *PLoS One* 6:e19477.
53. Chattopadhyaya B, et al. (2007) GAD67-mediated GABA synthesis and signaling regulate inhibitory synaptic innervation in the visual cortex. *Neuron* 54:889–903.
54. Chattopadhyaya B, et al. (2004) Experience and activity-dependent maturation of perisomatic GABAergic innervation in primary visual cortex during a postnatal critical period. *J Neurosci* 24:9598–9611.